Electron valence band of zirconium tetrafluoride

G. Kemister
La Trobe University, Bundoora, Victoria 3083, Australia

T. Warmiński*
Telstra Research Laboratories, 770 Blackburn Road, Clayton, Victoria 3168, Australia
(Received 7 August 1995; revised manuscript received 12 October 1995)

The partial *p*- and *d*-electron densities of states (DOS's) in the valence band of β-ZrF_4 were experimentally profiled through recording its Zr $M_{IV,V}$ and Zr L_{II} emission bands (spectra) by the x-ray spectrometer of an electron probe apparatus. *Ab initio* calculations were performed to determine the concentrations of individual F- and Zr-atom symmetry groups to the DOS and the number of states. The DOS maxima positions were found to correlate well with the measured peaks of the two bands.

I. INTRODUCTION

β-ZrF_4 is a volatile component of one group of so-called heavy metal fluoride (HMF) glasses, in which it typically comprises more than 50 mole % of their formulation.[1,2] HMF glasses are based on the binary system of β-ZrF_4 as the principal glass progenitor, and BaF_2 the principal modifier. The addition of further components, such as YF_3, InF_3, LaF_3, HF_4, and ThF_4 considerably stabilizes the glass without changing the basic optical properties. One of the unusual optical properties of these glasses, their midinfrared high transmission capability, is a phenomenon that holds a promise of ultralow loss transmission links. The present-day reason for the interest of the telecommunication industry in the glasses is mainly due to their low multiphonon absorption losses, which are lower by a factor of 10–100, in comparison with silica glasses. Consequently, the research on the glasses is proceeding towards a field of potential applications as 1.5 and 1.3 μm fiber amplifiers.[3,4]

Burbank and Bensey[5] found that the crystallographic structure of β-ZrF_4 consists of a three-dimensional array of antiprism polyhedra, which are joined together by the sharing of corners. Each Zr atom is coordinated by eight F atoms in the form of a square Archimedean antiprism, while each F atom is coordinated by two Zr atoms, with an average Zr-F distance of about 2.11 Å, and an average F-Zr-F angle of 75.4°. From the point of view of our present interest, it is important to emphasize that within the 60-atom unit cell of this compound, there are only two different symmetry positions, or types, for Zr atoms and seven positions for F atoms.

It is worth noting that the availability of good quality β-ZrF_4 crystals has been a restricting factor in the study of the material properties.[5] Our studies were not possible until 1987, when Robinson and Fuller[6] succeeded in growing centimeter size, clear and transparent crystals.

Section II presents an *ab initio* calculation of the electronic band of β-ZrF_4. Our idea was to simplify the calculations by compounding the partial contributions to the density of states (DOS) and number of states (NOS) of the highest energy band from the established F- and Zr-symmetry groups/units. Section III presents necessary details of x-ray spectroscopy measurements. We note that x-ray emission spectroscopy is capable of distinguishing between states having different symmetries. We include detailed information on the two zirconium spectra, Zr $M_{IV,V}$ and Zr L_{II}, which were only briefly shown in some previous publications,[7,8] and which are now playing a crucial role in verifying the theory. Section IV compares the experiment with the theory and Sec. V concludes the paper.

II. CALCULATION OF THE BAND STRUCTURE

Band calculations for simple crystals of diamond or zinc blende structures have developed to a stage where they can be considered as routine. Due to the large number of atoms in the unit cell of β-ZrF_4 the problem here is more involved. Density functional theory provides the basis for several computational schemes of solid state band structures. The most popular *ab initio* method for calculating electronic structure of crystals is the linear muffin-tin orbital (LMTO) approach, which is a local density formulation of the density functional theory. The LMTO approach assumes that each band in the crystal can be represented by a linear combination of atomic orbitals. We use the LMTO — atomic sphere approximation to the Hamiltonian.[9] The atomic sphere approximation assumes that the electron density around each atom is spherically symmetric inside a sphere of predetermined radius. This approximation works quite well for ionic crystals, such as β-ZrF_4. It reduces the complexity of the equations, especially for crystal unit cells of the size of β-ZrF_4, so that it is possible to solve them computationally.

From the inorganic database (I.C.S.D.) the dimensions of monoclinic β-ZrF_4, space group *C2/c*, are given as $a = 11.71$ Å, $b = 9.89$ Å, $c = 7.65$ Å, and $\beta = 126.15°$. The unit-cell dimensions of a sample of crystal of β-ZrF_4 supplied by Robinson of the Hughes Research Laboratories[6] were slightly different: $a = 11.794$ Å, $b = 9.946$ Å, $c = 7.703$ Å, $\beta = 126.13°$, and these values, consequently were used in our calculations. β-ZrF_4 has 12 Zr and 48 atoms in the unit cell; F^{-1} and Zr^{+4} atoms have the ionic radii of 1.36 Å and 0.80 Å, respectively.[10] Due to symmetry, some of the atoms are equivalent, and we have two different types of Zr and seven different types of F atoms. When enumerating the atoms, we follow the notation of Ref. 5. On the Zr side,

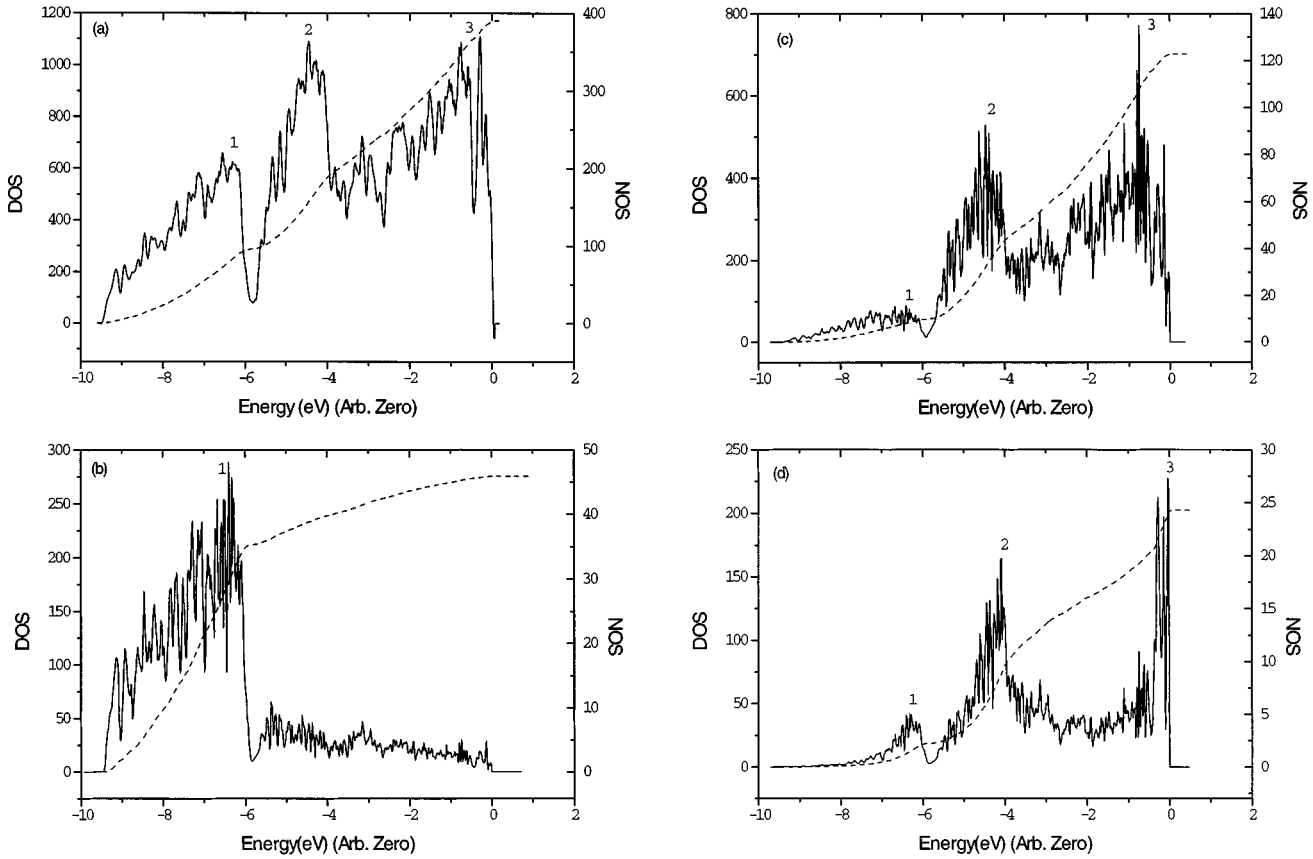

FIG. 1. The density of states (solid line), DOS, and the number of states (broken line), NOS, in the valence N band of β-ZrF_4: (a) the total picture (summary), (b) states filled by s electrons, (c) states filled by p electrons, and (d) states filled by d electrons. Numbers 1–3 indicate the DOS peaks (Table I).

the +4 ionization means loss of both 5p conducting electrons, plus, what is even more important for the Zr energy structure, the loss of the top two 4d electrons (out of eight comprising the Zr N shell). To form a heavily ionized core of Zr^{+4}, the neutral Zr atom undergoes a contraction by about 40%, and in the energy space a completely different 4th N shell, or the valence band of β-ZrF_4, is created.

A series of plots in Fig. 1 shows the electron densities and the number of states for the β-ZrF_4 valence band. In addition, Table I gives more detailed information on the different types of ionic contributions to the DOS peaks. There are three DOS peaks at the following binding energies: 1:[− 6.3eV], 2:[−(4.1, 4.5) eV], 3:[−(0.0, 0.7) eV]. As the bands in the calculations are made up of linear combinations of atomic orbitals, the densities of states can be separated into partial densities of state for each atomic orbital.

Table II gives the identification of major Zr and F contributions to the peaks. The lowest energy peak consists of mostly s contributions, and thus it represents the N_{I} shell (subband). Two middle peaks have both p- and d-like symmetry contributions, and they are energetically almost indistinguishable. They are the degenerate shells of $N_{\mathrm{II-V}}$. It is interesting to note that the top of the $N_{\mathrm{IV,V}}$ shell, as well as the top of the β-ZrF_4 valence band, is made up of 4d electrons of Zr and 2p electrons of F atoms. The degeneracy of the p- and d-electron contributions may be partially due to the atomic sphere approximation, which ensures that the p- and d-electron densities are spherically symmetric, thereby removing any chance of splitting the levels by directionality effects. This approximation may also have the effect of

TABLE I. Computed electron contributions of Zr and F atoms into the valence N band of β-ZrF_4 in the percentage values of the total DOS.

Energy space		F atoms							Zr atoms	
Electrons	DOS peak	1	2	3	4	5	6	7	1	2
4s	1	9	14	16	17	14	14	16		
	1	6	5	15	15	17	12	15	6	9
4p	2	11	6	17	16	14	15	12	3	6
	3	7	7	21	15	16	17	17		
	1								41	59
4d	2								29	71
	3								16	84

TABLE II. Major contributions of Zr and F atoms to the N band of of β-ZrF_4.

Subband	DOS peak : [eV]	Major contribution
N_{I}	1 : [-6.3]	Zr 4s, Zr 4p, F 2s
$N_{\mathrm{II,III}}$	2 : [-4.5]	Zr 4s, Zr 4p, Zr 4d, F 2p
$N_{\mathrm{IV,V}}$	2 : [-4.1]	Zr 4s, Zr 4p, Zr 4d, F 2p
$N_{\mathrm{II,III}}$	3 : [-0.7]	Zr 4d, F 2p
$N_{\mathrm{IV,V}}$	3 : [-(0,0.5)]	Zr 4d, F 2p

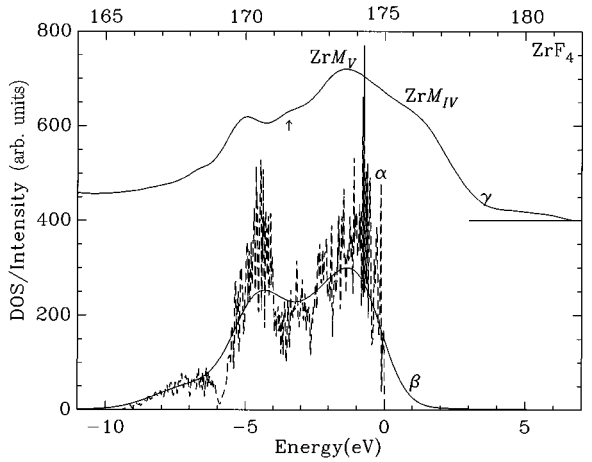

FIG. 2. The Zr $M_{\mathrm{IV,V}}$ emission band of β-ZrF_4 crystal: α — the 4p-electron DOS, β — the smeared 4p-electron DOS, and γ — the experimental spectrum filtered from about 2k spectral points (its energy scale is given at the top).

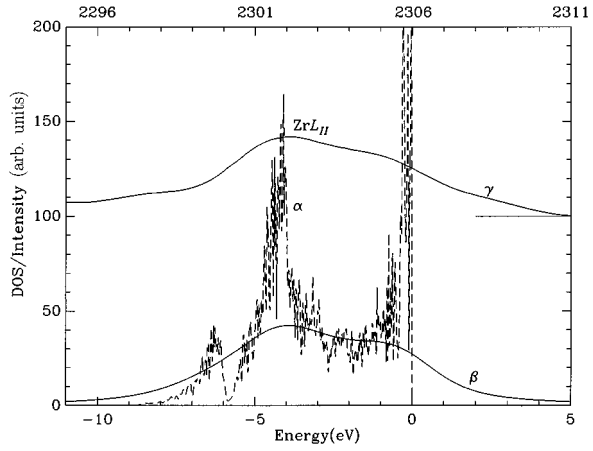

FIG. 3. The Zr L_{II} emission band of β-ZrF_4 crystal: α — the 4d-electron DOS, β — the smeared 4d-electron DOS, and γ — the experimental spectrum after numerical filtration (its energy scale is given at the top).

smearing out these peaks to some extent. Hence, it is not possible for us to identify any angular symmetry effects within the DOS plots.

III. X-RAY EMISSION SPECTROSCOPY

X-ray emission spectroscopy has the unique ability of testing symmetries of selected pairs of the electron states (initial, final), which are involved in producing x-ray photons. A valence state can be an initial state with any core level allowed by the selection rules being the other component of the pair. In contrast, x-ray photoelectron spectroscopy (XPS), which is a surface characterization technique, is not efficient in providing recovery of a partial density of states from XPS valence band spectra.[11,12]

Various wavelength dispersive spectrometers can be used in x-ray emission spectroscopy. We operate a regular single-crystal Johann-type spectrometer with 140 mm Rowland circle of an electron probe apparatus.[7]

Spectroscopic (i.e., nonconventional nonanalytical) studies of materials by an electron probe technique are handicapped by the fact that one has to record large volumes of spectral data. For example, insulators require a typical low counting rate of about 10 counts per second for a large number of points, so it takes many hours to complete a single spectrum. The low counting rate for insulating materials has a serious consequence on the quality of the spectral results, i.e., poor signal to noise ratios.[13] To enhance clarity of the microprobe recorded curves, we typically transform our data into the frequency domain, perform a near-rectangular frequency domain filtering, and transform them back to the energy domain.

In this work, we concentrate on two very weak x-ray emission bands (spectra), i.e., $M_{\mathrm{IV,V}}$ and L_{II} of zirconium. If measured on β-ZrF_4, the intensity of a strong analytical line of Zr $L\alpha_{1,2}$ is about 90 and 170 times stronger than the peak intensities of Zr $M_{\mathrm{IV,V}}$ and Zr L_{II} bands, respectively. The typical settings for the spectra recording had been 10 keV and 30 nA. They are presented as noise-filtered plots γ, at the top of Figs. 2 and 3. Also, to indicate some similarities of the shape features, the DOS peaks α, and the ''smeared'' DOS peaks β from Fig. 1 are reproduced at their bottoms. The x-ray and the DOS energy scales have been matched by aligning the positions of the main maximum at 173.6 eV, and that of the 3rd peak in the β characteristic.

Figure 4 shows the smearing functions, convolutions of Lorentzian and Gaussian, which have been used to smooth the DOS peaks. First, spectroscopic linewidths are determined by the lifetimes of the initial and final states. In zirconium, the natural widths of the $M_{\mathrm{IV,V}}$ and L_{II} core levels are approximately 0.2 and 2 eV, respectively.[14] Those are represented as the half widths of the Lorentzian part of the smearing functions. However, the Zr $M_{\mathrm{IV,V}}$ spectrum is mostly broadened by a large energetic separation of its two components, i.e., the M_{IV} and M_{V} spectra and this effect was not included to the functions. Second, the spectrum is also broadened by the spectrometer, and as we used a single-crystal one, there is an extra width added which is indepen-

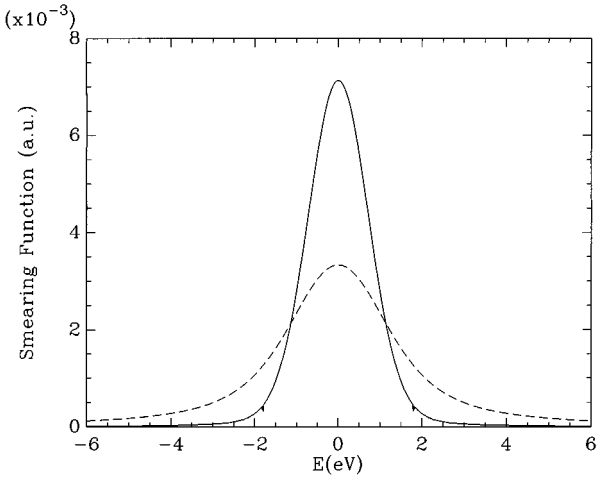

FIG. 4. The smearing functions used in this work to smooth the 4p-electron DOS (solid line), and the 4d-electron DOS (broken line); the narrower one is effectively Gaussian and the wider has the Lorentzian character.

dent of the wavelengths.[15] We used the $M_{IV,V}$ maximum from Zr metal at 151.1 eV,[16] with a narrow full width at half maximum width of 0.77 eV,[17] in order to obtain an estimated value for the broadening. In our experimental setup of the spectrometer a widely open slit of 3 mm has been used with the high analyzer crystal positions of around 200 mm, producing an effective broadening (or resolution reduction) of 1.6 eV. The slit broadening is represented as the half width of the Gaussian part of the smearing functions.

IV. COMPARISON WITH THEORY

Figure 2 shows the Zr $M_{IV,V}$ emission band for β-ZrF_4 single crystal with the DOS plot for p electrons. This spectrum represents the hole transition of the type $3d_{3/2}d_{5/2}$ $(M_{IV,V}) \rightarrow 4p_{1/2},p_{3/2}$ $(N_{II,III})$. The energy of this transition for β-ZrF_4 is smaller than the energy of the corresponding transition of $M_{IV,V}O_{II,III}$ for Zr metal.[18,8] There are clearly some maxima on the Zr $M_{IV,V}$ spectrum. The three maxima, which form the Zr M_V emission band, can be correlated with three peaks on the DOS plot for p electrons (as their energy positions and not heights are concerned). By looking into the percentage contributions from different atoms to the DOS peaks (Table I), we can conclude that all fluorine atoms contribute to the density of states of all these maxima, most contributions coming from types 3 through 7. The zirconium atoms participate in the formation of the first and second maxima. The fourth maximum can be seen on the energy tail of the third (main) maximum, from which it is separated by about 2.5 eV. Because of the 2.3(4) eV energy difference of $M_{IV,V}$ levels (or 3d levels),[19,20] it seems appropriate to identify this additional maximum as the Zr M_{IV} emission band of β-ZrF_4. It could also be true that a kink marked by an arrow in Fig. 2, is due to a second DOS peak contribution to that band.

It is difficult to quantify the agreement between the Zr $M_{IV,V}$ spectrum and the DOS calculations, simply because not all the empirical factors, which could influence the exact maxima heights and positions, could have been evaluated. In general, however, the agreement is satisfactory. The theory predicts a slightly smaller separation of the two main peaks, as well a somewhat bigger ratio of the heights of the smaller to the higher.

The Zr L_{II} spectrum is shown in Fig. 3. It is generated as a result of the $2p_{1/2} \rightarrow 4d_{3/2}$ hole transition, or $L_{II}N_{IV}$ one (not $L_{III}N_{IV}$ as it was claimed in Ref. 7). Again, maxima of this spectrum and those of the smeared DOS d-electron plot agree reasonably well. Although the energies of the Zr M_V and L_{II} spectra are very different, they can be aligned by subtracting the energies of the appropriate core levels. It turns out that the separation distance between the main maxima of these spectra is about 1 eV. Within the experimental error, it is roughly the same as the calculated difference in the energies of the second and third peaks for the DOS d- and p-electron plots, which according to our prediction are shifted by about 0.5 eV.

The contribution of β-ZrF_4 d electrons from the smaller (but narrower) second DOS peak to the Zr L_{II} spectrum seems to be stronger than that of the higher third DOS peak, however, in a smeared form, the positions and the ratio of the second to the third DOS peaks are almost identical as those for the maxima on the measured spectrum.

In Zr metal the energetically degenerated $4d_{3/2},d_{5/2}$ levels have a binding of 3 eV, and with their involvement, the hole transition from the L_{II} level is producing a single maximum at 2304 eV. In β-ZrF_4 the analogous transition is at 2302 eV, suggesting that the binding energy increases to about 5 eV [which is in agreement with the position of the second DOS peak on the d-electrons plot of Fig. 1(d)].

V. CONCLUSIONS

The zirconium $M_{IV,V}$ and L_{II} spectra of β-ZrF_4 agree with our computed model of the β-ZrF_4 electronic band structure. Thus, we predict, with a high degree of confidence, that the top of β-ZrF_4 valence band is constructed from 4d electrons of Zr atoms, mostly of type 2, and from the 2p electrons of all the F atoms. We also predict that the maxima of 4s and 4p electrons are created from mixed contributions of all seven types of F atoms. Since the short range order of the ionic arrangements in the β-ZrF_4 crystal and in the fluorozirconate glasses are similar, we anticipate the usefulness of the present results to the glass domain as well. Predictions are that the glasses are built of just a limited number of different configurational Zr-F atomic arrangements, and some of them are those which make partial contributions to the crystal of β-ZrF_4.

ACKNOWLEDGMENTS

A helpful assistance of A. Duncan at the spectra recording and processing is acknowledged. The samples of β-ZrF_4 crystals were supplied by M. Robinson of Hughes Research Laboratories, at Malibu, California. We are indebted to J. Szymański for his valuable comments.

*Author to whom the correspondence should be addressed.

[1] *Fluoride Glass Fibre Optics*, edited by I.D. Aggarwal and G. Lu (Academic Press, San Diego, 1991).

[2] P.W. France, M.G. Drexhage, J.M. Parker, M.W. Moore, S.F. Carter, and J.V. Wright, *Fluoride Glass Optical Fibres* (Blackie, Glasgow, 1990).

[3] W.J. Miniscalco, Tech. Dig. Ser. **13**, 44 (1991).

[4] M. Brierley, *Progress on Optical Amplifiers for 1.3μm*, Optical & Photonics News, January 1992, p. 15.

[5] R.D. Burbank and F.N. Bensey, Jr., *The Crystal Structure of Zirconium Tetrafluoride*, *USA-EC Rept* (Union Carbide Nuclear Co., Union Carbide and Carbon Corp., Oak Ridge, Tennessee, 1956).

[6] M. Robinson and K.C. Fuller, Mater. Res. Bull. **22**, 1725 (1987).

[7] T. Warmiński and A. Duncan, Mater. Sci. Forum C **67&68**, 437 (1991).

[8] T. Warmiński and A. Duncan, *Collected Abstracts of the XVth Congress and General Assembly of International Union of Crystallography, Bordeaux, France, 1990* (IUCR, Bordeaux, 1990).

[9] N.E. Christensen, Phys. Rev. B **30**, 5753 (1984); T. Brudevoll, D.S. Citrin, M. Cardona, and N.E. Christensen, *ibid.* **48**, 8629 (1993).

[10] *Van Nostrand Reinhold Encyclopedia of Chemistry*, 4th ed., edited by D.M. Considine and G.D. Considine (Van Nostrand Reinhold, New York, 1984), pp. 216 and 220.
[11] W. Kolas and L. Wolniewicz, J. Chem. Phys. **24**, 457 (1974).
[12] M.L. Ristig, Nucl. Phys. A **317**, 163 (1979).
[13] J.W. Colby, in *Proceedings of the 6th International Conference on X-Ray Optics and Microanalysis*, edited by G. Shinoda, K. Khora, and T. Ichinokawa (University of Tokyo Press, Tokyo, 1972), p. 247; also in *Practical Scanning Electron Microscopy*, edited by J.I. Goldstein and H. Yakowitz (Plenum Press, New York, 1975), Chap. XII, p. 465.
[14] K.D. Sevier, *Low Energy Electron Spectroscopy* (Wiley, New York, 1972), Chap. 6, p. 234, Fig. 6.
[15] L.V. Azároff, *X-Ray Spectroscopy* (McGraw-Hill, New York, 1974), Chaps. II.C, III.F, V.I-J.
[16] J.A. Beardon (unpublished).
[17] J.C. Rivière, in *Practical Surface Analysis by Auger and X-ray Photoelectron Spectroscopy*, edited by D. Briggs and M.P. Seah (Wiley, New York, 1983), Chap. 2, p. 50, Table 2.1.
[18] J. Holliday, in *Handbook of X-Rays*, edited by E. Keable (McGraw-Hill, New York, 1967), Chap. 38; also in *Characterization of Solid Surfaces*, edited by Ph.F. Kane and G.B. Larrabee (Plenum, New York, 1976), Chap. 19, p. 495.
[19] J.A. Bearden and A.F. Burr, Rev. Mod. Phys. **39**, 125 (1967).
[20] J.C. Fuggle and A.F. Burr, J. Electron Spectrosc. **21**, 275 (1980).